Ceramics-Silikáty 67 (1), 73-80 (2023)
www.ceramics-silikaty.cz doi: 10.13168/cs.2023.0004

EFFECT OF REPLACEMENT OF CaO BY La_2O_3 ON THE STRUCTURE, THERMAL AND DIELECTRIC PROPERTIES OF ALKALI-FREE ALUMINOBOROSILICATE GLASSES

WENXU WU, XIAOKUN TIAN*, LULU ZHANG*, XIN LIU*, CHAO WU*, GUOXUAN GU*, YA QU*, XUNMEI LIANG**, #YUNLONG YUE*, #JUNFENG KANG**

**School of Materials Science and Engineering, University of Jinan, Jinan, China*
***Taian Road Engineering Materials Co., Ltd, Taian, China*

#E-mail: zztg_yueyl@163.com, mse_kangjf@ujn.edu.cn

Submitted December 13, 2022; accepted January 30, 2023

Keywords: Aluminoborosilicate glasses, Lanthanum oxide, Thermal expansion, Thermal stability, Dielectric properties

Alkali-free aluminoborosilicate glasses were prepared by the conventional melting method. The effect of the replacement of CaO by La_2O_3 on the structure, thermal, and dielectric properties of the glasses was investigated by FTIR, DSC, with thermal expansion instruments, and an impedance analyser. With increasing ratios of La_2O_3 to CaO, the densities of the glasses increased linearly from 2.458 to 2.627 g·cm^{-3}. Meanwhile, the polymerisation degree of the glass network increased first and then decreased. The glass transition temperature, crystallisation onset temperature and expansion softening temperature showed a gradually increasing trend, while the thermal stability firstly deteriorated, then gradually improved. Additionally, the coefficient of thermal expansion (CTE), dielectric constant and dielectric loss initially decreased, followed by an increase. The sample with the La_2O_3/CaO ratio of 1.00 showed excellent properties: had a low CTE (2.71 × 10^{-6} °C^{-1}), had a dielectric constant (5.23), and a dielectric loss (1.12 × 10^{-3}), which means it is a promising material for integrated circuit packaging applications.

INTRODUCTION

Integrated circuit (IC) packaging is developing towards high density interconnections, with the prospect of thinner packaging and higher routing density [1]. However, traditional organic substrates face several challenges, such as warpage, material dimensional stability issues in manufacturing and high-density inputs/outputs (I/Os) with very fine line interconnections. Glass fibre fabrics have superior properties to other substrate materials, such as having a high insulation ability, an adjustable coefficient of thermal expansion (CTE) matching that of the silicon material, a low dielectric constant and loss. Therefore, glass fibre fabrics have become an attractive candidate in the IC substrate industry to replace the intermediate layer materials [2-6]. The glass fibres currently available for electronic printed circuit boards are E-glass fibre, L-glass fibre, S-glass fibre, and T-glass fibre. However, the glass fibre for the IC substrate must have a lower CTE to match that of the silicon material (~2.5 × 10^{-6} °C^{-1}) to neutralise the thermal stress generated by the thermal expansion in the glass and prevent spalling during heat treatment. The thermal expansion properties of the above glass fibres (CTE > 3.5 × 10^{-6} °C^{-1}) are far from that of the silicon material, so they need to be improved to better meet the application requirement [6].

The glass fibre for the IC substrate mainly belongs to the alkali-free aluminoborosilicate glass system due to its good dielectric properties and thermal stability. Rare earth oxides have a remarkable impact upon the structure and performance in silicate glass systems. Hence, in order to improve some properties of alkali-free aluminoborosilicate glass, rare earth oxides, as network modifiers, are usually regarded as effective additives [7-17]. Gao et al [18] found that the substitution of Y_2O_3 for Al_2O_3 showed a strong effect on the structure and properties of alkali-free aluminoborosilicate glasses. The density and CTE of glasses increased by the incorporation of Y_2O_3. Li et al [19] showed and discussed the aluminoborosilicate glasses containing La_2O_3 and CeO_2. The results showed that more Q^3 and Q^4 are formed in the samples with the La_2O_3/RE_xO_y ratio of 1/2, meaning that the structure is the most compact. Meanwhile, the best dielectric properties were obtained here.

Taking the above into account, this paper aims to investigate the effects on the structure, thermal expansion properties, thermal stability, dielectric properties of the alkali-free aluminoborosilicate glasses with the replacement of CaO by La_2O_3.

EXPERIMENTAL

Preparation of glass

The chemical compositions of the studied glasses are shown in Table 1. The glass samples were labelled as L1, L2, L3, L4, L5, and L6, respectively, with the La_2O_3/ /CaO ratio increasing from 0 to 2.50. All the glass batches were weighed precisely and mixed thoroughly. Then the homogeneous mixtures were melted in a platinum-rhodium crucible for 3 - 6 h at temperatures between 1580 and 1650 °C in a high-temperature furnace, depending on the composition. The homogenised melts were dumped on the preheated graphite plate mould. The obtained glass cubes were transferred to a muffle furnace immediately after solidification. The glass samples were annealed at 780 - 800 °C for 2 - 3 h to release the stress, then cooled in the furnace.

Sample characterisation

According to Archimedes' principle, the density of the glass was gauged using an electronic analytical balance (AR223CN, Ohaus Co., Ltd). The deionised water at room temperature was selected as the immersion liquid. To improve the accuracy, the average value per sample was metred three times to eliminate errors in the measurement. According to the calculation, the density error was within 0.014 $g \cdot cm^{-3}$.

The infrared (IR) spectra of the glass were measured through the KBr disc technique by an infrared spectrometer (Nicolet iS10, Thermo Fisher Scientific, USA) with a resolution was 0.5 cm^{-1} in the range of 400 - 2000 cm^{-1}. The glass sample was ground to a fine powder using an agate mortar. The homogeneous mixing ratio of glass powder to KBr powder was 1:100.

The differential scanning calorimetry (DSC) analysis of the glass was characterised using a Mettler-Toledo Thermal Analyser (TGA/DSC 1600HT). The glass sample powder was manually ground in the agate mortar and then placed in a 70 μL corundum crucible. The reference matter was a high-purity Al_2O_3 powder. The specimen was controlled when heating from 50 °C to 1400 °C at 10 °C min^{-1}. The characteristic temperatures were obtained with an error of 1 °C.

The dilatometric experiment was performed using a horizontal push-rod expansion instrument (Orton DIL 1412STD, USA) from 25 °C to 900 °C with a controlled heating rate of 5 $°C \cdot min^{-1}$ in an air atmosphere. Thermal expansion properties are critical for glass, which is defined as the change in the rate of the length of the glass sample from L1 to L2 when the temperature rises from T1 to T2. The glass sample was made in dimensions of size 4 × 4 × 25.4 mm. It is noteworthy that both ends of the specimen rod were sandpapered. The coefficient of thermal expansion (CTE) is the average linear expansion coefficient and can be evaluated as per the formula below:

$$\alpha = \frac{L_2 - L_1}{L_1 (T_2 - T_1)} \quad (1)$$

where L_1 is the length of the glass sample at temperature T_1 and L_2 is the length of the glass sample at temperature T_2.

The dielectric property of the glass was measured using an impedance analyser (Keysight E4990A) with a matching 16451B fixture at 1 MHz at room temperature and air atmosphere. The glass sample was cut into a rectangle measuring 10 × 10 × 2 mm using automatic cutting equipment and polished by a metallographic grinding machine. The dielectric constant (ε) and dielectric loss (tan α) can be directly obtained from the analysis of the instrument's software.

RESULTS AND DISCUSSION

Density

The density of the glasses with different La_2O_3/CaO ratios are shown in Figure 1. Obviously, the densities of the glasses were linearly dependent on the La_2O_3/ /CaO ratio. The glass density rose linearly from 2.458 to 2.627 $g \cdot cm^{-3}$ with an increase in the La_2O_3/CaO ratio from 0 to 2.50. The glass density is determined primarily by the chemical composition, precisely, the atomic masses of its components [20, 21]. In terms of the atomic mass of the elements in the studied compositions, the atomic mass of La^{3+} (138.905) is much larger than that of the Ca^{2+} (40.078), and the density of the glasses increased significantly with the replacement of CaO by La_2O_3.

Table 1. Chemical composition of various glass samples (mol. %)

Glass samples	Al_2O_3	SiO_2	B_2O_3	MgO	CaO	La_2O_3	La_2O_3/ CaO
L1	18	64	6	6	6	0	0.00
L2	18	64	6	6	5	0.5	0.10
L3	18	64	6	6	4	1.0	0.25
L4	18	64	6	6	3	1.5	0.50
L5	18	64	6	6	2	2.0	1.00
L6	18	64	6	6	1	2.5	2.50

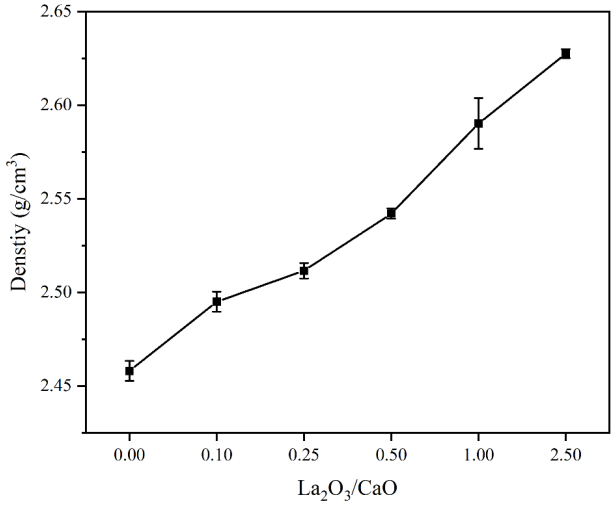

Figure 1. Density as a function of the La_2O_3/CaO ratio

Infrared spectra

The Fourier-transform infrared (FTIR) spectroscopy curves of the aluminoborosilicate glasses with the replacement of CaO by La_2O_3 are depicted in Figure 2. The increase in the replacement CaO by La_2O_3 had an effect on the infrared spectrum, and five characteristic absorption peaks can clearly be observed. The absorption peak around 450 cm^{-1} is responsible for the bending vibration of Si-O in [SiO_4] [22], and the peak located at 687 cm^{-1} is ascribed to the vibration of the Si-O-Al connected [SiO_4] and [AlO_4] tetrahedra structure units [23, 24]. The absorption peak near 790 cm^{-1} is due to the stretching vibration of the Al-O in the [AlO_4] tetrahedron or the symmetric stretching vibration of the Si-O-Al bond [25, 26]. The peak which occurs at 1086 cm^{-1} is attributed to the asymmetric stretching vibration of the Si-O in [SiO_4] or the stretching vibration of the B-O-B bond in the [BO_4] tetrahedron [27, 28]. The peak at about 1420 cm^{-1} may correspond to the asymmetric stretching vibration of B-O in the [BO_3] triangle [29].

The absorption peak around 1420 cm^{-1} moved to the lower band first with the increase in the La_2O_3/CaO ratio from 0 to 1.00 and then shifted to the higher band. The former may be due to the increase in the free oxygens with the replacement of CaO by La_2O_3, resulting in the conversion of [BO_3] to [BO_4]. The latter may be due to the increase in the [BO_3] content with the excessive La_2O_3 content [17]. Obviously, the positions of the other four absorption peaks exhibited the same change trend just opposite to that of around 1420 cm^{-1}, i.e., moving first to the higher wavenumber and then shifting to the lower wavenumber. The peak near 1086 cm^{-1} moved to a higher band and then shifted to the lower band with the increase in the La_2O_3/CaO ratio. The reason is that free oxygens increased with the increase in the La_2O_3/CaO ratio (below 1.00), which would diminish the quantity of the non-bridging oxygen (NBO) in [SiO_4] and boost the conversion of [BO_3] to [BO_4], causing the enhancement of the glass network polymerisation [30]. Meanwhile, the broad wave number range of 850 - 1200 cm^{-1} can be deconvoluted by the Gaussian method as shown in Figure 3 and described by Si-O_b utilising the Q^n family (n = 1,2,3,4, number of BO atoms) as shown in Figure 4. The particulars of the Q^n family are shown in Table 2. The value of the total amount of Q^3 and Q^4 decreased first and then increased, indicating that the connectivity of the network structure first enhanced and then diminished while the La_2O_3/CaO ratio rose from 0 to 2.50. The peak near 687 cm^{-1} and 790 cm^{-1} moved to a higher wavenumber while the La_2O_3/CaO ratio increased from 0 to 1.00, and then decreased. The former indicated that the increase in the connections among the [SiO_4] tetrahedra and between the [SiO_4] and [AlO_4] tetrahedra [31], and reached the maximum polymerisation degree at the La_2O_3/CaO ratio of 1.00.

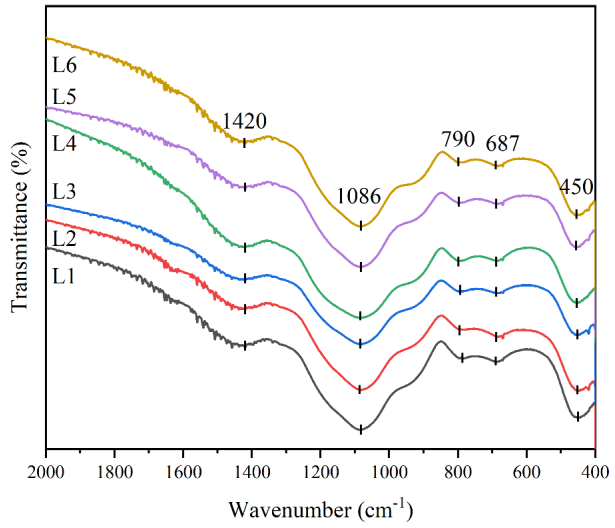

Figure 2. FTIR curves of the aluminoborosilicate glasses with the replacement of CaO by La_2O_3.

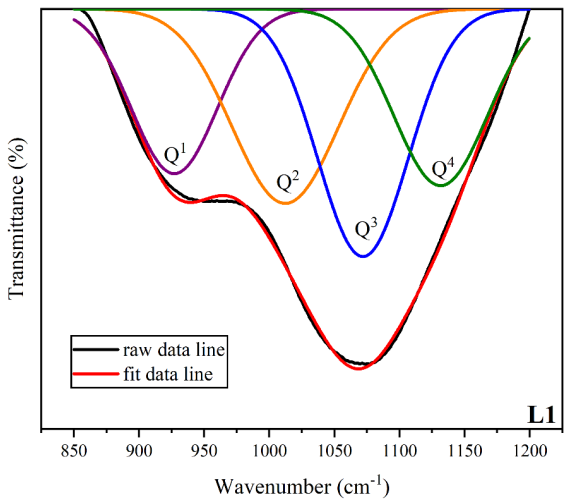

Figure 3. The deconvolution curve of L1 with the Gaussian function. The black line refers to the raw data line and the red line refers to the fit data line.

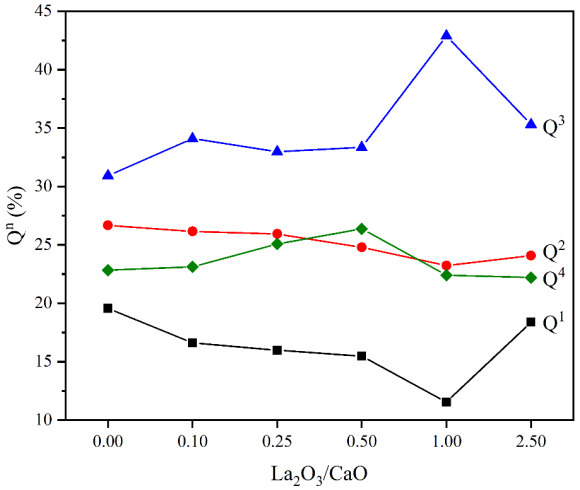

Figure 4. Area percentage of Q^n (n = 1, 2, 3, 4) for the glass samples deconvolved from the Gaussian function.

Table 2. Area percentage of Q^n of the glasses.

Glass samples	L1	L2	L3	L4	L5	L6
Q^1 (%)	19.57	16.61	15.99	15.48	11.54	18.39
Q^2 (%)	26.67	26.16	25.94	24.79	23.23	24.09
Q^3 (%)	30.93	34.10	32.99	33.35	42.90	35.31
Q^4 (%)	22.84	23.13	25.08	26.38	22.41	22.20
$Q^3 + Q^4$ (%)	53.76	57.23	58.07	59.73	65.31	51.56

Subsequently, the degree of polymerisation decreased with the excessive La_2O_3 content.

Thermal properties

The DSC graphs of the glasses are shown in Figure 5. The glass transition temperature (T_g) and crystallisation onset temperature (T_c) exhibited a gradually increasing trend, while the thermal stability firstly deteriorated, then gradually improved. In addition, the crystallisation peak temperature (T_p) first decreased and then increased gradually.

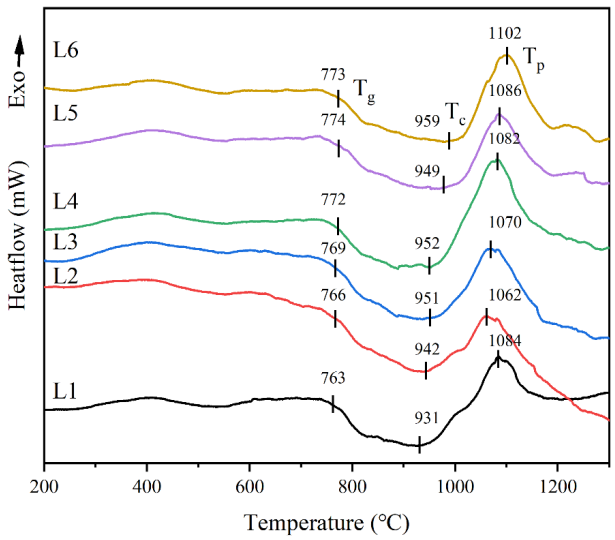

Figure 5. DSC curve of the aluminoborosilicate glasses with the replacement of CaO by La_2O_3.

The thermal stability of the glasses was illustrated according to the given parameters ΔT and S by Dietzal [32] and Saad-Paulin[33], respectively:

Dietzal: $$\Delta T = T_p - T_g \quad (4)$$

Saad-Paulin: $$S = \frac{(T_p - T_c)(T_c - T_g)}{T_g} \quad (5)$$

Three characteristic temperatures and two thermal stability parameters of the glasses extracted from the DSC graphs are summarised in Table 3. ΔT represents the capacity of the molten glass for resisting the crystallisation and maintaining the amorphous phase as it cools and solidifies. Moreover, S is the capacity of the glass to resist devitrification after the glass formation. The larger the ΔT and S values are, the stronger the glass formation ability is [17, 34, 35]. When the La_2O_3/CaO ratio was 2.50, the ΔT and S reached the maximum value, indicating that the most stable glass formed in the studied compositions.

Table 3. The characteristic temperatures and thermal stability parameters of the glasses.

sample number	T_g	T_c	T_p	ΔT	S
L1	763	931	1084	321	33.69
L2	766	942	1062	296	27.57
L3	769	951	1070	301	28.16
L4	772	952	1082	310	30.31
L5	774	949	1086	312	30.98
L6	773	959	1102	329	34.41

The coefficient of thermal expansion

As the temperature increases, the thermal motion amplitude of the particles in the glass also increases, resulting in larger particle spacing and the external manifestation is expansion [36-39]. The effect of the different La_2O_3/CaO ratios on the thermal expansion characteristics of the studied glasses are shown in Figure 6. The CTE, T_g', and expansion softening temperature (T_f) of the glasses were determined from the dilatometric curves registered in Figure 6, and the outcomes are outlined in Table 4.

The CTE is largely governed by the chemical composition of the glass which is also affected by the selected temperature range [40]. The former mainly affects the thermal expansion property by its formed structure in the glass. According to the needs of the application scenario, the final CTE value was obtained by calculating the average value over the temperature range of 50 - 300 °C, as shown in Figure 7. With the increased La_2O_3/CaO ratio from 0 to 2.50, the T_g' and

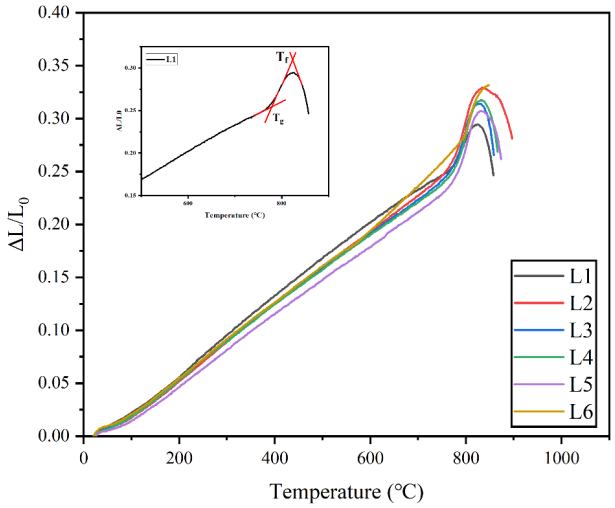

Figure 6. Thermal expansion curves of the glasses with the replacement of CaO by La_2O_3.

Table 4. Coefficient of thermal expansion, transition and expansion softening temperature of the glasses.

Sample ID	CTE(50-300 °C) ($\times 10^{-6}$ °C^{-1})	T_g' ± 2.0 (°C)	T_f ± 0.5 (°C)
L1	3.08 ± 0.01	757.4	828.3
L2	2.97 ± 0.03	755.8	836.8
L3	2.94 ± 0.02	755.1	832.6
L4	2.87 ± 0.01	768.0	835.3
L5	2.71 ± 0.03	774.9	842.4
L6	2.91 ± 0.03	773.6	848.9

T_f gradually increased over the studied compositions. The CTE decreased initially, followed by an increase. The sample with the La_2O_3/CaO ratio of 1.00 showed excellent thermal expansion properties, with the CTE of the glass sample being 2.71×10^{-6} °C^{-1}. Therefore, it can match well with silicon materials due to its excellent thermal expansion properties, i.e., a lower CTE close to that of the silicon material. The decrease in the CTE correlated with the improvement in the aggregation degree of the network structure. When the La_2O_3/CaO ratio increased from 0 to 1.00, the more free oxygen led to a decrease in the amount of NBO in [SiO_4], resulting in the reduction in the average asymmetry of the network structure. Then the CTE increased due to the structure disrupted by the excessive free oxygen, resulting in an increase in the unsaturated silicon-oxygen bond and strengthening the disconnection of the network structure in the glass [18]. This is closely related to the rare earth oxide La_2O_3, which is similar to an alkaline earth metal oxide, playing a dominant role in destroying the network structure by acting as a modifier oxide when the La_2O_3/CaO ratio exceeds 1.00. In addition, the relatively larger radius of La^{3+} would elicit a definite degree of deformation in the network structure with further La_2O_3/CaO growth. The deformed network structure is more susceptible to vibrations during heat treatment, thereby leading to an increase in CTE [37].

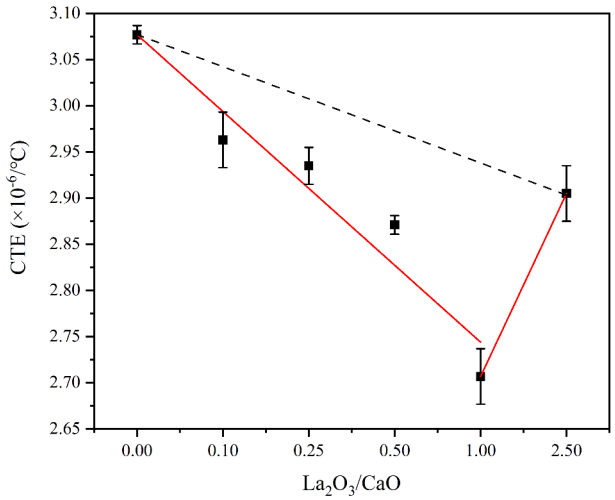

Figure 7. CTE as a function of the La_2O_3/CaO(the solid line). The CTE was obtained by taking the average value between 50 and 300 °C. The dashed line refers to the linear relationship between the two ends of the components. The solid lines represent the apparent association between the CTE and the components. The two lines are both guides for the eyes.

Dielectric properties

The dielectric properties of the studied glasses with the different La_2O_3/CaO ratios are shown in Figure 8. The dielectric constant (ε) is mainly affected by the ionic polarisability and mobility. The dielectric loss (tan α) is principally determined by the space charge polarisation and ionic migration loss [19, 41]. The dielectric constant and dielectric loss firstly deteriorated and then improved. The sample with the La_2O_3/CaO ratio of 1.00 showed excellent dielectric properties, and the values of the dielectric constant and loss are 5.23 and 1.12×10^{-3}, respectively. The replacement of CaO by La_2O_3 has a mixed intermediate effect similar to that of the "mixed alkali effect" in which case the substitution of two oxides result

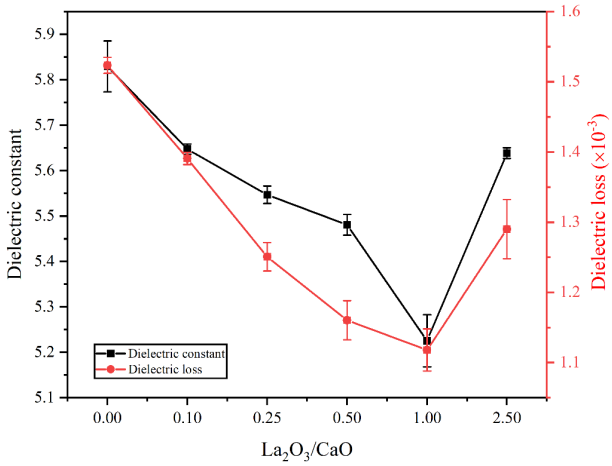

Figure 8. Dielectric constant and dielectric loss of the aluminoborosilicate glasses under a 1 MHz electric field at room temperature.

in the occurrence of an extreme value in the properties of the components. This could be intimately correlated with the different effects of the La_2O_3 and CaO contributions to the glass structure [10, 13, 42].

The field strength of La^{3+} is weaker on the account of its larger ionic radius than Ca^{2+} (La^{3+}:1.061Å, Ca^{2+}:0.99Å). The network structure becomes more compact due to less attraction from the rare earth oxide (La_2O_3), indicating that the higher the La_2O_3/CaO ratio (below 1.00) the less NBO [15, 31]. Meanwhile, the lower ionic polarisability of La^{3+} than that of Ca^{2+} has a positive effect on reducing the dielectric constant [43]. On the other hand, the larger ionic radius of La^{3+} became more difficult to migrate in an increasingly compact network structure, resulting in the reduction of ε and tan α. Therefore, the ε and tan α gradually decreased with the La_2O_3/CaO ratio increasing from 0 to 1.00. When the ratio of La_2O_3/CaO further increased, the ion migration and space charge polarisation increased with a diminish in the polymerisation degree of the network structure, increasing the dielectric constant and loss.

CONCLUSION

In this paper, the replacement of CaO by La_2O_3 has a significant impact on the structure, thermal expansion properties, thermal stability, and dielectric properties of the studied glasses. The results revealed that the replacement of CaO by La_2O_3 enhanced the density of the glass significantly. When the La_2O_3/CaO ratio increased from 0 to 2.50, the densities of the glasses increased linearly from 2.46 to 2.68 $g \cdot cm^{-3}$. Meanwhile, the polymerisation degree of the glass network increased and then decreased. When the La_2O_3/CaO ratio was 1.00, the polymerisation degree of the glass network reached the highest value. While the network structure was disrupted by the excessive non-bridging oxygen with a further increase in the La_2O_3/CaO ratio, resulting in lower totals for Q^3 and Q^4. As for the thermal properties, T_g and T_c exhibited a gradually increasing trend, while the thermal stability firstly deteriorated, then gradually improved. In addition, the coefficient of thermal expansion (CTE), dielectric constant, and dielectric loss decreased initially, followed by an increase. The sample with a La_2O_3/CaO ratio of 1.00 exhibited excellent properties: had a lower CTE (2.71×10^{-6} $°C^{-1}$), a dielectric constant (5.23), and a dielectric loss (1.12×10^{-3}), which shows it is a promising material as an IC substrate for IC packaging applications.

Acknowledgement

This work was supported by the National Natural Science Foundation of China (NSFC) with grant numbers 51872117, 51672105, 52172019, 52072148, and the Opening Project of State Key Laboratory of Advanced Technology for Float Glass (No. 2020KF01). The authors appreciate the help of other teachers for the measurements in the School of Material Science and Engineering, University of Jinan.

REFERENCES

1. Ilderem V. (2020): The technology underpinning 5G. *Nature Electronics, 3*(1), 5-6. Doi:10.1038/s41928-019-0363-6
2. Chien C. H., Chen C. C., Yeh W. L., Lin W. T., Wu C. H., Chen F. Y., et al. (2019). Study Photo Imagable dielectric (PID) and non-PID on process, fabrication and reliability by using panel glass substrate for next generation interconnection. In: *International Symposium on Microelectronics* (Vol. 2019, No. 1, pp. 000216-000222). International Microelectronics Assembly and Packaging Society.Doi: 10.4071/2380-4505-2019.1.000216
3. Chen Y. H., Hsu S., Ra, U., Shenoy R., Lai K. Y., Shorey A. B., et al. (2014). Low cost glass interposer development. In: *International symposium on microelectronics* (Vol. 2014, No. 1, pp. 000397-000401). International Microelectronics Assembly and Packaging Society.Doi:10.4071/isom-WA15
4. Shorey A., Cochet P., Huffman A., Keech J., Lueck M., Pollard S., Ruhmer K. (2014). Advancements in fabrication of glass interposers. In: *2014 IEEE 64th Electronic Components and Technology Conference (ECTC)* (pp. 20-25). IEEE. Doi: 10.1109/ECTC.2014.6897261
5. Muguruma T., Behr A., Saito H., Kishino K., Suzuki F., Shin T., Umehara H. (2022). Low-Dielectric, Low-Profile IC Substrate Material Development for 5G Applications. In: *2022 IEEE 72nd Electronic Components and Technology Conference (ECTC)* (pp. 56-61). IEEE. Doi: 10.1109/ECTC51906.2022.00017
6. Selvanayagam C. S., Lau J. H., Zhang X., Seah S. K. W., Vaidyanathan K., Chai T. C. (2009): Nonlinear thermal stress/strain analyses of copper filled TSV (through silicon via) and their flip-chip microbumps. *IEEE transactions on advanced packaging, 32*(4), 720-728. Doi: 10.1109/TADVP.2009.2021661
7. Olin P. H., Wolff J. A. (2012): Partitioning of rare earth and high field strength elements between titanite and phonolitic liquid. *Lithos, 128*, 46-54.Doi: 10.1016/j.lithos.2011.10.007
8. Dan H. K., Ty N. M., Tap T. D., Vinh H. X., Vinh L. T., Jiao Q., et al. (2019): Effects of Al^{3+}/La^{3+} ratio on the DSC/DTA and luminescence properties of Bi-doped lanthanum aluminosilicate glasses. *Infrared Physics & Technology, 103*, 103072.Doi:10.1016/j.infrared.2019.103072
9. Lu Y., Liu H., Qu Y., Lu H., Huang S., Yue Y. (2017): Influence of La_2O_3 and Ce_2O_3 additions on structure and properties of aluminoborosilicate glasses. *Journal of Materials Science: Materials in Electronics, 28*, 2716-2722. Doi: 10.1007/s10854-016-5850-1
10. Zhao J., Lu Y., Kang J., Qu Y., Khater G. A., Li S., et al. (2018): Effect of Y_2O_3 and La_2O_3 on structure and dielectric properties of aluminoborosilicate glasses. *Journal of Non-Crystalline Solids, 496*, 1-5.Doi: 10.1016/j.jnoncrysol.2018.05.020
11. Li Y., Zhang T., Feng Y., Liu C., Jiang M. (2020): Liquid regions of lanthanum-bearing aluminosilicates. *Materials,*

13(2), 450.Doi: 10.3390/ma13020450
12. Wang M.T., Fang L., Mei L.I., Liu Z.G., Yan-Hong H.U., Zhang X.W. (2017): Effect of Rare Earth Dopant on Thermal Stability and Structure of ZnO-B_2O_3-SiO_2 Glass. *International Journal of Inorganic Materials, 32*(6), 643-648. Doi:10.15541/jim20160509
13. Wang M. T., Cheng J. S., Li M., He F. (2011): Structure and properties of soda lime silicate glass doped with rare earth. *Physica B: Condensed Matter, 406*(2), 187-191. Doi: 10.1016/j.physb.2010.10.040
14. Guo W., Ding Z., Wang J., Wu J., Wang Z. (2021): Effect of La_2O_3 on the viscosity and structure of CaO-SiO_2(-Al_2O_3)-La_2O_3 melts. *Materials Chemistry and Physics, 266,* 124526. Doi: 10.1016/j.matchemphys.2021.124526
15. Zhang X. H., Yue Y. L., Wu H. T. (2012): Influence of La_2O_3 additions on chemical durability and dielectric properties of boroaluminosilicate glasses. *Surface Review and Letters, 19*(06), 1250062. Doi: 10.1142/S0218625X1250062X
16. Wang X., Hu L., Meng X., Li H., Wang S. (2018): Effect of Al_2O_3 and La_2O_3 on structure and spectroscopic properties of Nd-doped sol–gel silica glasses. *Journal of Luminescence, 204*, 554-559. Doi: 10.1016/j.jlumin.2018.08.015
17. Zhang L., Kang J., Wang J., Khater G. A., Shi Q., Li S., et al. (2019): Effects of Y_2O_3 on structure and dielectric properties of aluminoborosilicate glasses. *Journal of Non-Crystalline Solids, 503*, 110-114.Doi: 10.1016/j.jnoncrysol.2018.09.032
18. Gao X., Zhang Q., Yu J., Tang W., Li Y., Lu A. (2018): Effect of replacement of Al_2O_3 by Y_2O_3 on the structure and properties of alkali-free boro-aluminosilicate glass. *Journal of Non-Crystalline Solids, 481*, 98-102. Doi: 10.1016/j.jnoncrysol.2017.10.032
19. Li S., Lu Y., Qu Y., Kang J., Yue Y., Liang X. (2021): Dielectric and thermal properties of aluminoborosilicate glasses doped with mixed rare-earth oxides. *Journal of Non-Crystalline Solids, 556*, 120550. Doi: 10.1016/j.jnoncrysol.2020.120550
20. Hager I. Z., El-Mallawany R. (2010): Preparation and structural studies in the $(70-x)TeO_2$–$20WO_3$–$10Li_2O$–xLn_2O_3 glasses. *Journal of Materials Science, 45*, 897-905. Doi: 10.1007/s10853-009-4017-3
21. Zamyatin O. A., Plekhovich A. D., Zamyatina E. V., Sibirkin A. A. (2016): Glass-forming region and physical properties of the glasses in the TeO_2−MoO_3 − Bi_2O_3 system. *Journal of Non-Crystalline Solids, 452*, 130-135.Doi: 10.1016/j.jnoncrysol.2016.08.027
22. Salama S.N., Salman S.M., Darwish H. (2002): Effect of nucleation catalysts on crystallisation characteristics of aluminosilicate glasses. *Ceramics-Silikáty 46*(1),15-23.
23. Cheng J., Xiao Z., Yang K., Wu H. (2013): Viscosity, fragility and structure of Na_2O–CaO–Al_2O_3–SiO_2 glasses of increasing Al/Si ratio. *Ceramics International, 39*(4), 4055-4062. Doi: 10.1016/j.ceramint.2012.10.258
24. Hamilton J. P., Brantley S. L., Pantano C. G., Criscenti L. J., Kubicki J. D. (2001): Dissolution of nepheline, jadeite and albite glasses: toward better models for aluminosilicate dissolution. *Geochimica et Cosmochimica Acta, 65*(21), 3683-3702. Doi:10.1016/S0016-7037(01)00724-4
25. Cheng Y., Xiao H., Shuguang C., Tang B. (2009): Structure and crystallization of B_2O_3–Al_2O_3–SiO_2 glasses. *Physica B: Condensed Matter, 404*(8-11), 1230-1234. Doi:10.1016/j.physb.2008.11.198
26. Xie J., Xiao Z. F., Zheng W. H., Liu Y., Cheng J. S. (2012). The effect of Al_2O_3/SiO_2 on the structure and properties of Na_2O-CaO-Al_2O_3-SiO_2 glasses. In: *Key Engineering Materials* (Vol. 509, pp. 339-345). Trans Tech Publications Ltd.Doi:10.4028/www.scientific.net/KEM.509.339
27.] Huang C., Behrman E. C. (1991): Structure and properties of calcium aluminosilicate glasses. *Journal of Non-Crystalline Solids, 128*(3), 310-321.Doi:10.1016/0022-3093(91)90468-L
28. Hao X., Luo Z., Hu X., Song J., Tang Y., Lu A. (2016): Effect of replacement of B_2O_3 by ZnO on preparation and properties of transparent cordierite-based glass-ceramics. *Journal of Non-Crystalline Solids, 432*, 265-270. Doi:10.1016/j.jnoncrysol.2015.10.017
29. Kamitsos E. I., Karakassides M. A., Chryssikos G. D. (1987): A vibrational study of lithium borate glasses with high Li_2O content. *Physics and Chemistry of Glasses, 28*(5), 203-209.
30. Lu Y., Liu H., Qu Y., Lu H., Huang S., Yue Y. (2017): Influence of La_2O_3 and Ce_2O_3 additions on structure and properties of aluminoborosilicate glasses. *Journal of Materials Science: Materials in Electronics, 28*, 2716-2722.Doi:10.1007/s10854-016-5850-1
31. Okuno M., Zotov N., Schmücker M., Schneider H. (2005): Structure of SiO_2–Al_2O_3 glasses: combined X-ray diffraction, IR and Raman studies. *Journal of Non-Crystalline Solids, 351*(12-13), 1032-1038.Doi:10.1016/j.jnoncrysol.2005.01.014
32. Dietzel A. (1968): Glass structure and glass properties. *Glasstech, 22,* 41.
33. Saad M., Poulain M. (1987). Glass forming ability criterion. In *Materials science forum* (Vol. 19, pp. 11-18). Trans Tech Publications Ltd. Doi: 10.4028/www.scientific.net/MSF.19-20.11
34. Huang Q., Liu J., He X., Liu T., Lu A. (2021): Analysis of structure evolution and performance in alkali-free glass substrates via XPS and infrared: Boron-aluminum anomaly. *Journal of Non-Crystalline Solids, 555*, 120531. Doi: 10.1016/j.jnoncrysol.2020.120531
35. Gui H., Li C., Lin C., Zhang Q., Luo Z., Han L., et al. (2019): Glass forming, crystallization, and physical properties of MgO-Al_2O_3-SiO_2-B_2O_3 glass-ceramics modified by ZnO replacing MgO. *Journal of the European Ceramic Society, 39*(4), 1397-1410.Doi: 10.1016/j.jeurceramsoc.2018.10.002
36. Darwish H., Gomaa M. (2006): Effect of compositional changes on the structure and properties of alkali-alumino borosilicate glasses. *Journal of Materials Science: Materials in Electronics, 17,* 35-43. Doi: 10.1007/s10854-005-5139-2
37. Wang W., Cao Z., Du R., Ruan J., Wang J., Liu C., et al. (2019): Structure and properties of non-alkali aluminoborosilicate glass containing RE (RE= La, Ce, Nd, Dy, Y, Yb) oxides. *Journal of Non-Crystalline Solids, 516*, 45-49. Doi:10.1016/j.jnoncrysol.2019.04.031
38. Lofaj F., Satet R., Hoffmann M. J., de Arellano Lopez A. R. (2004): Thermal expansion and glass transition temperature of the rare-earth doped oxynitride glasses. *Journal of the European Ceramic Society, 24*(12), 3377-3385. Doi: 10.1016/j.jeurceramsoc.2003.10.012
39. Hampshire S., Drew R. A., Jack K. H. (1984): Viscosities, Glass Transition Temperatures, and Microhardness of Y-Si-A1-O-N Glasses. *Journal of the American Ceramic Society, 67*(3), C-46. Doi: 10.1111/j.1151-2916.1984.tb19752.x

40. Shelby J. E. (2020). *Introduction to glass science and technology.* Royal society of chemistry.
41. Yue Y. L., Yu X. J., Wu H. T., Chen X. J. (2009): Dielectric properties of quaternary calcium aluminoborosilicate system glasses. *Materials Research Innovations, 13*(2), 129-132.Doi: 10.1179/143307509X435141
42. Kjeldsen J., Smedskjaer M. M., Mauro J. C., Youngman R. E., Huang L., Yue Y. (2013): Mixed alkaline earth effect in sodium aluminosilicate glasses. *Journal of Non-Crystalline Solids, 369*, 61-68. Doi: 10.1016/j.jnoncrysol.2013.03.015
43. Iftekhar S., Grins J., Edén M. (2010): Composition–property relationships of the La_2O_3–Al_2O_3–SiO_2 glass system. *Journal of Non-Crystalline Solids, 356*(20-22), 1043-1048.Doi: 10.1016/j.jnoncrysol.2010.01.017